HHS Public Access

Author manuscript

J Comp Neurol. Author manuscript; available in PMC 2016 October 15.

Published in final edited form as:

J Comp Neurol. 2015 October 15; 523(15): 2254–2271. doi:10.1002/cne.23787.

Cerebellar premotor output neurons collateralize to innervate the cerebellar cortex

Brenda D. Houck and **Abigail L. Person**

Department of Physiology & Biophysics, University of Colorado School of Medicine Aurora, CO 80045

Abstract

Motor commands computed by the cerebellum are hypothesized to use corollary discharge, or copies of outgoing commands, to accelerate motor corrections. Identifying sources of corollary discharge, therefore, is critical for testing this hypothesis. Here, we verified that the pathway from the cerebellar nuclei to the cerebellar cortex in mice includes collaterals of cerebellar premotor output neurons, mapped this collateral pathway, and identified its postsynaptic targets. Following bidirectional tracer injections into a distal target of the cerebellar nuclei, the ventrolateral thalamus, we observed retrogradely labeled somata in the cerebellar nuclei and mossy fiber terminals in the cerebellar granule layer, consistent with collateral branching. Corroborating these observations, bidirectional tracer injections into the cerebellar cortex retrogradely labeled somata in the cerebellar nuclei and boutons in the ventrolateral thalamus. To test whether nuclear output neurons projecting to the red nucleus also collateralize to the cerebellar cortex, we used a Cre-dependent viral approach, avoiding potential confounds of direct red nucleus-to-cerebellum projections. Injections of a Cre-dependent GFP-expressing virus into Ntsr1-Cre mice, which express Cre selectively in the cerebellar nuclei, retrogradely labeled somata in the interposed nucleus and putative collateral branches terminating as mossy fibers in the cerebellar cortex. Postsynaptic targets of all labeled mossy fiber terminals were identified using immunohistochemical Golgi cell markers and electron microscopic profiles of granule cells, indicating that the collaterals of nuclear output neurons contact both Golgi and granule cells. These results clarify the organization of a subset of nucleocortical projections which constitute an experimentally accessible corollary discharge pathway within the cerebellum.

Keywords

Corollary discharge; efference copy; interposed; motor coordination; Purkinje; RRIDs: AB_2315383; AB_2315774; AB_528480; AB_10307; AB_91937; AB_10566289; AB_10051818; AB_143165; AB_10054551; AB_305564

Address for Correspondence: Abigail L. Person, Department of Physiology & Biophysics, University of Colorado School of Medicine, 12800 East 19th Ave, RC-1 North, Campus Box 8307, Aurora, CO 80045, USA, abigail.person@ucdenver.edu, (303) 724-4514.

Conflict of Interest: The authors declare no competing financial interests.

Role of Authors: All authors had full access to all the data in the study and take responsibility for the integrity of the data and the accuracy of the data analysis. Study concept and design: Brenda Houck, Abigail Person. Acquisition of data: BH. Analysis and interpretation of data: BH, AP. Drafting of the manuscript: BH, AP. Critical revision of the manuscript for important intellectual content: BH, AP. Statistical analysis: BH, AP. Obtained funding: AP. Administrative, technical, and material support: AP. Study supervision: BH, AP.

Introduction

Although the cerebellum is widely recognized to support coordinated movements and motor learning, its mechanistic role in these behaviors remains enigmatic (Ito, 1984). Theoretical models propose that the cerebellum improves movements by computing feedforward signals in which internal feedback, and specifically corollary discharge, is used to guide motor output (Kawato and Gomi, 1992; Miall et al., 1993; Wolpert, 1997; Wolpert et al., 1998; Ohyama et al., 2003; Shadmehr and Krakauer, 2008; Lisberger, 2009). Despite this important role for corollary discharge, little is known about the source of such information in the cerebellum.

One candidate source of corollary discharge to the cerebellar cortex is from the cerebellar nuclei (CbN), which drive movements via projections to premotor structures such as the red nucleus, reticular formation and ventrolateral thalamus (Chan-Palay, 1977; Mauk and Thompson, 1987; Hesslow, 1994). A pathway from the CbN to the granule cell layer has been identified, but a systematic examination of collaterals of premotor CbN principle neurons, thus constituting a corollary discharge pathway, had not been performed. The cerebellar nuclei contain at least three cell types: glutamatergic premotor principle output neurons, GABAergic and glycinergic interneurons, and GABAergic nucleo-olivary neurons (Chan-Palay, 1977; Uusisaari and Knöpfel, 2010; Husson et al., 2014). This cellular diversity underlines the importance of isolating specific nucleocortical populations for examination.

The nucleocortical pathway was initially identified in cats with retrograde and anterograde methods (Gould and Graybiel, 1976; Tolbert et al., 1976). Subsequently, this tract was further characterized across many species including primates, pigeons, rats and mice (Clarke, 1977; Tolbert et al., 1977, 1980; Chan-Palay et al., 1979; Hendelman and Marshall, 1980). It is thought to include axons of all types of nuclear neurons (Chan-Palay, 1977; Chan-Palay et al., 1979; Hámori and Takács, 1989; Batini et al., 1992; Kolston et al., 1995; Angaut et al., 1996; Uusisaari and Knöpfel, 2010). Antidromic stimulation and intracellular recording studies suggest that at least some of the nucleocortical pathway is composed of axon collaterals of cerebellar premotor output neurons (Tolbert et al., 1976, 1978; McCrea et al., 1978) and anatomical evidence exists for collateralization of CbN output neurons to ventrolateral thalamus and red nucleus target areas (Shinoda et al., 1988). Together these two lines of research suggest that CbN output neurons may provide motor command feedback through the nucleocortical pathway. Such an input to the cerebellar cortex could serve as a source of rapid motor feedback to sculpt cerebellar-dependent movements (Wolpert et al., 1998; Shadmehr and Krakauer, 2008; Lisberger, 2009).

Here we address the question of whether cerebellar output neurons provide internal feedback via collaterals to the cerebellar cortex and if so which cells this pathway targets. Using a combination of bidirectional tracers and immunolabeling in wildtype and transgenic mice, our data clarify an anatomical pathway within the cerebellum well suited to provide corollary discharge information to the granule cell layer.

Materials and Methods

Subjects

Adult C57/B6 (Charles River), Neurotensin receptor1-Cre (Ntsr1-Cre; Mutant Mouse Regional Resource Center ; STOCK Tg(Ntsr1-cre)GN220Gsat/Mmucd), Rosa26-tdTomato (B6.129S6-Gt(ROSA)26Sor$^{tm14(CAG-tdTomato)Hze}$/J, Jackson Laboratory) and GlyT2-GFP mice (Salk Institute; Zeilhofer et al., 2005; Tg(Slc6a5-EGFP)13Uze) of either sex were used in accordance with the National Institutes of Health Guidelines and the Institutional Animal Care and Use Committee at the University of Colorado Anschutz Medical Campus. Animals were housed in an environmentally-controlled room, kept on a 12:12 light/dark cycle and had *ad libitum* access to food and water. Crosses of the Ntsr1-Cre and Rosa26-tdTomato reporter mice were used in preliminary experiments to assess the distribution of Cre expression in the cerebellum and midbrain.

Biotinylated Dextran Amine Injections

For all surgical procedures mice were anesthetized with intraperitoneal injections of a Ketamine Hydrochloride (100 mg/kg) and Xylazine (10 mg/kg) cocktail, placed in a stereotaxic apparatus and prepared for surgery with a scalp incision. Craniotomies were made above the ventrolateral nucleus of the thalamus (2–3 injections from bregma: 0.6, 0.8, 1.0 mm posterior, 1.0 mm lateral, 3.3 mm ventral; n=11 C57/B6 mice, n=4 GlyT2-GFP mice), the cerebellar cortex (anterior injection targeting the putative region involved in delay eyelid conditioning behavior (DEC; Heiney et al., 2014; Steinmetz and Freeman, 2014), from lambda: 1.6 mm posterior, 2.0 mm lateral, 1.6–1.8 mm ventral; n=4 mice; posterior injection, from lambda: 2.0 mm posterior, 2.3 mm lateral, 1.0 mm ventral; n=5 mice), the cerebellar nuclei (CbN; 1 injection from lambda: 2.0mm posterior, 1.0 mm lateral, 2.5 ventral; n=5 mice) or the red nucleus (2 injections from bregma: 3.4, 3.6 mm posterior, 0.6 lateral, 3.6 mm ventral; n=9 mice). Iontophoretic injections of 10% 10-kDa biotinylated dextran amine (BDA; Invitrogen) were administered using a pulled glass pipette (30–40 μm tip diameter) at 5–6.5 μA for 8–10 minutes and a 50:50 duty cycle. Mice were allowed to survive for 11–16 days before perfusion.

Virus Injections

Craniotomies were made above the red nucleus in Ntsr1-Cre mice as described above. Bilateral pressure injections of 0.15–0.25 μL AAV1.CAG.Flex.eGFP.WRPRE.bGH (AAV1.Flex.eGFP; Penn Vector Core, Gene Therapy Program, University of Pennsylvania; n=4 mice) were made using a 1μL Hamilton Neuros syringe attached to the stereotaxic apparatus (Hamilton). All mice were housed postoperatively for 3 weeks before perfusion to allow for viral expression throughout the entirety of the axonal arbor.

Tissue Preparation for Light Microscopy

Mice were overdosed with an intraperitoneal (IP) injection of a sodium pentobarbital solution, Fatal Plus (Vortech Pharmaceuticals), and perfused transcardially with 0.9% saline followed by either 4% paraformaldehyde or, for tissue used in electron microscopy, a 4% paraformaldehyde/1% gluteraldehyde solution in 0.1M phosphate buffer (PB). Brains were

removed and postfixed for at least 24 hours then cryoprotected in 30% sucrose. Brains were sliced in 40 μm serial coronal sections using a freezing microtome and stored in PB.

Immunohistochemistry

Floating sections spanning the forebrain to brainstem were rinsed in 0.3% Triton X-100 in PB (1hr; Sigma-Aldrich). In a subset of cases a permeabilization solution was used to increase tissue penetration (1hr; consisting of 0.1M PB, 0.15M NaCl, 0.3% Triton X-100, and 1% Bovine Serum Albumin). To visualize BDA, sections were incubated with Streptavidin conjugated to Alexa Fluor 488 (Life Technologies; Cat# S32354; RRID: AB_2315383), Alexa Fluor 555 (Life Technologies; Cat# S32355) or Alexa Fluor 568 (Life Technologies; Cat# S11226; RRID: AB_2315774) at a 1:100 dilution in PB for two hours followed by three washes in PB (10 min each). For immunolabeling, sections were blocked in a solution of 10% Normal Goat Serum (Invitrogen) in PB or in the permeabilization solution described above (1hr) and then incubated with one or two of the following primary antibodies (host in parenthesis): (mouse) Synaptic Vesicle Protein 2 (SV2; Developmental Studies Hybridoma Bank Cat# sv2, RRID:AB_528480; for 48 hours at 1:400; concentration determined from serial dilution test); (rabbit) anti-metabotropic Glutamate receptor 2+3 (mGluR 2/3; Abcam; Cat# ab6438, Lot# GR12051, RRID: AB_10307; manufacturer recommended dilution) for 24–48 hours at 1:500; (rabbit) anti-neurogranin for 24 hours at 1:500 (Millipore; Cat#AB5620, Lot# 2441899; RRID: AB_91937; manufacturer recommended dilution) (Table 1).

After three washes in PB, sections were then incubated with secondary antibodies at a 1:400 dilution (90 min). The secondary antibodies used included goat anti-mouse IgG Alexa Fluor 488 (Invitrogen; Cat# A-11001; RRID: AB_10566289) or 405 (Invitrogen; Cat# A-31553; RRID: AB_10051818) and goat anti-rabbit IgG Alexa Fluor 488 (Molecular Probes; Cat# A-11008; RRID: AB_143165) or 405 (Invitrogen; Cat# A-31556; RRID: AB_10054551). In double label experiments, BDA was developed after immunolabeling. Following three rinses in PB, sections were mounted onto slides and coverslipped using Fluoromount-G (SouthernBiotech). A subset of tissue from specimen with BDA injections to the ventrolateral thalamus was processed for Nissl by incubating in a 1:500 dilution of Neurotrace Fluorescent Nissl stain (Life Technologies; Cat# N-21479; concentration determined from serial dilution) for 20 min followed by a 10 minute rinse in PB with 0.3% Triton X.

Antibody Characterization

Antibody sources and epitope information is summarized in Table 1. The SV2 antibody was a monoclonal antibody developed by Dr. Kathleen Buckley (University of California, San Francisco) and was obtained from the Developmental Studies Hybridoma Bank, created by the NICHD of the NIH and maintained at The University of Iowa, Department of Biology, Iowa City, IA. The SV2 antibody was raised against synaptic vesicles from the *Ommata* electric organ and binds to a transmembrane glycoprotein of ~95 kDa on the cytoplasmic side of synaptic vesicles (Buckley and Kelly, 1985; manufacturer specifications). The mGluR 2/3 polyclonal antibody was raised against a synthetic peptide (NGREVVDSTTSSL) corresponding to the 13 c-terminus amino acids of mGluR2 and 3 in

rat with an N-appended lysine coupled to thyroglobulin using gluteraldehyde (manufacturer specifications). The neurogranin polyclonal antibody was raised against the recombinant rat neurogranin (complete sequence; manufacturer specifications). Published descriptions (Simat et al., 2007) of Golgi cell staining patterns with mGluR2/3 and neurogranin antibodies were corroborated in our hands, supportive of antibody specificity. Furthermore, we confirmed specificity of the secondary antibodies by processing a subset of tissue in the absence of primary antibody that resulted in no cellular label.

Processing for Electron Microscopy

Coronal cerebellar sections from Ntsr1-Cre mice with injections of AAV.Flex.eGFP into the red nucleus were rinsed three times, 10 minutes each in 0.1M Phosphate Buffered Saline (PBS). To permeate cell membranes, tissue was placed in a freeze-thaw solution (0.2M PB, sucrose, glycerol) for 20 minutes and then moved to a mixture containing 50% freeze-thaw solution and 50% 0.1M PBS in an Eppendorf tube for three freeze-thaw cycles in liquid nitrogen. Following one 10 minute rinse in PBS, sections were then blocked in 10% NGS and 3% BSA in 0.1M PBS for one hour. Sections were incubated with a rabbit polyclonal primary anti-GFP antibody (1:50; Abcam; Cat# AB6556; RRID: AB_305564) (Table 1) for 24 hours at 4°C, washed in 0.1M PBS (3 times, 10 min), then reacted with a biotinylated Goat anti-Rabbit IgG secondary antibody (1:200 in 0.1M PBS; Jackson ImmunoResearch) before a final set of rinses (3 times in PBS, 10 min). Tissue was incubated in ABC peroxidase reagent complex (Vector) overnight at 4°C then washed before reacting in 0.05% DAB in 0.05M Tris Buffer for 10 minutes. Hydrogen peroxide (0.003%) was added to visualize DAB labeled cells. Reactions were quenched by washing tissue in PBS.

Slices were embedded in 5% agarose in 0.1 M phosphate buffer and trimmed to the region with DAB-labeled processes. Sections were rinsed in 100 mM cacodylate buffer and then immersed in 1% osmium and 1.5% potassium ferrocyanide for 15 min to enhance membrane contrast (Rivlin and Raymond, 1987), rinsed five times in cacodylate buffer, immersed in 1% osmium for 1 hour, and then rinsed again five times for 2 min each in cacodylate buffer and two times briefly in water. Slices were then transferred to graded ethanols (50, 70, 90, and 100%) containing 2% uranyl acetate for 15 minutes each. Finally, slices were transferred through propylene oxide at room temperature and then embedded in LX112 (Electron Microscopy Sciences #RT14120) and cured for 48 h at 60°C in an oven (modified from Harris et al., 2006).

Ultra-thin sections (50 nm) were cut on a Reichert Ultracut E from a small trapezoid positioned over DAB labeled mossy fiber rosettes in the granule cell layer of the cerebellar cortex and were picked up on Formvar-coated slot grids (EMS). Sections were imaged on a FEI Technai G2 transmission electron microscope with a Gatan UltraScan 1000 digital camera at magnifications ranging from 1,200x to 4,800x. Pixel intensity histograms were adjusted using Adobe Photoshop CS6.

Imaging

Confocal images of immunolabeled sections were obtained using either a Zeiss Axioskop 2 running LSM5 Pascal or a Zeiss Observer.Z1 3i Marianas Spinning Disk microscope

equipped with an Evolve camera running Slidebook software (Intelligent Innovations). Pixel intensity histograms were adjusted using ImageJ and Adobe Photoshop CS6.

Terminal Quantification and Mapping

For quantification, label was analyzed with a Zeiss Axiovert 135TV microscope with HBO 100W lamp. Mossy fiber terminals were identified as a large swelling surrounded by four to twelve knob-like outgrowths in the granule cell layer connected to an axon. Labeled somata were counted within the boundaries of the cerebellar nuclei. Terminals and somata were counted in every third section (approximately 120 μm increments) encompassing the anterior-posterior length of the cerebellum. Quantification and location of labeled terminals were mapped onto atlas landmarks (Paxinos and Franklin, 2008). Size measurements were made on micrographs collected with 63X (1.4 NA) and 100X (1.4 NA) objectives. N's in the text indicate numbers of mice unless noted otherwise.

Results

Ventrolateral thalamus injections label nucleocortical collaterals

To determine if nuclear premotor output neurons collateralize to innervate the granule cell layer, we injected bidirectional tracer into the ventrolateral thalamus. We predicted that if CbN projection neurons collateralize to the cerebellar cortex, such tracer injections would label terminals in the granule cell layer. Iontophoretic injections of 10-kDa BDA into the ventrolateral thalamus (n=11; Fig. 1A,B) yielded retrogradely labeled somata in the contralateral CbN (Fig. 1D; 2N) as well as axons coursing up to and forming mossy fibers in the granule cell layer of several cerebellar lobules, including Simple and Crus 1 (Fig. 1E; 2M; lobules specified in Fig 4, see below), consistent with the idea that cerebellar nuclear output neurons collateralize to innervate the granule cell layer. Following ventrolateral thalamus injections, little if any retrograde label was observed outside of the CbN with none observed in the following precerebellar nuclei: inferior olive, red nucleus (magnocellular and parvocellular), reticular formation (including lateral reticular nucleus, reticulotegmental nucleus of the pons, paramedian reticular nucleus), pontine nuclei (Fu et al., 2011). Importantly, any somatic label outside of the CbN was sparse and inconsistent. For instance, retrograde label was found in three cells in the gigantocellular reticular nucleus (n=2/11 mice), four cells in the mesencephalic reticular formation (n=3/11 mice), two cells in the pretectal nucleus (n=1/11 mice) and six cells in the substantia nigra reticularis (n=2/11 mice). Thus, the mossy fiber terminals described below are likely terminals of nuclear output neuron collaterals.

As mentioned above, retrograde somatic label following ventrolateral thalamus injections was mainly restricted to the dentate, both anterior and posterior interposed and fastigial cerebellar nuclei. This observation permitted us to investigate potential collateralization of cerebellar output neurons to other brainstem and midbrain targets by examining the tissue for terminal arborizations outside of the cerebellum. Following ventrolateral thalamus injections, boutons in the red nucleus ipsilateral to the injection site were consistently labeled (Fig. 1C; 2O). Two possibilities could account for this label. First, the ventrolateral thalamus could project directly to the red nucleus. Second, nuclear output neurons could

collateralize to innervate both the red nucleus and ventrolateral thalamus. To distinguish these possibilities, we injected the red nucleus directly with BDA. Following red nucleus injections, no retrograde label was observed in the ventrolateral thalamus, consistent with the view that labeled red nucleus boutons following ventrolateral thalamus injections were collaterals of CbN output neurons (n=9/9 mice).

As expected, ventrolateral thalamus injections consistently labeled terminals in primary motor cortex (n=10/10 mice for which there was tissue). In addition, terminals were also labeled less consistently in the following regions: medullary reticular nucleus (n=1/11 mice); tegmental nucleus (n=2/11 mice); pontine nucleus (n=1/11 mice); mesencephalic reticular formation (n=5/11 mice); superior colliculus (n=3/11 mice); inferior colliculus (n=1/11); visual cortex (n=2/11 mice); auditory cortex (n=1/11 mice); entorhinal cortex (n=1/11 mice); periaqueductal gray (n=3/11 mice); hypothalamic nucleus (n=1/11 mice); zona incerta (n=3/11 mice); dysgranular cortex (n=2/11 mice); granular cortex (n=1/11 mice); thalamic nuclei (n=2/11 mice); association cortices (n=2/11 mice); somatosensory cortices (n=1/11 mice); pontine nucleus oralis (n=1/11 mice).

Matched terminal fields following granule layer and CbN BDA injections

Further evidence that CbN output neurons collateralize to multiple targets including the granule cell layer, red nucleus and ventrolateral thalamus, was derived from injections of each of these areas in turn. These injections revealed consistent areas of somatic and terminal label, which are displayed in a matrix of images (Fig. 2) organized by injection sites (rows) and locations of tracer label (columns). BDA injections were made in the longitudinal zones C1, C2 and C3 of the cerebellar cortex, including the granule cell layer at the boundary between Simple and Lobule 6 (Fig. 2A). These injections retrogradely labeled somata in the anterior interposed nucleus, consistent with reports of topographical organization of the nucleocortical pathway in other species (n=5/6; Fig. 2B; Gould and Graybiel, 1976; Tolbert et al., 1976; Dietrichs and Walberg, 1979, 1980) and the general topographic arrangement of mossy fiber and intracerebellar organization (Oberdick and Sillitoe, 2011). Injections that retrogradely labeled somata in the CbN also labeled axons and terminals but not somata in the contralateral ventrolateral thalamus and red nucleus (n=9; Fig. 2C,D), consistent with branching fibers.

Tracer injections made into the interposed nucleus (anterior and posterior) (n=6) provided additional evidence for collateralization of CbN output neurons as reported in previous studies (McCrea et al., 1978; Shinoda et al., 1988), labeling both mossy fiber rosettes in the granule cell layer of Simple, Crus I, Crus II and 4/5 lobules (Fig. 2E) and axons branching and ramifying within the red nucleus (Fig. 2G). These axons appeared to continue coursing dorsally out of the red nucleus toward the thalamus. Terminals in the ventrolateral thalamus following both granule layer injections and CbN injections had unique boutonal morphology with a grape-like appearance (Fig. 2H). The long axis of these terminals ranged from 2.69–10.67 μm with a mean of 4.96 μm ± 0.19 and the short axis ranged from 1.67–6.75 μm with a mean of 3.08 μm ± 0.11 (n=73 terminals).

Taken together, results from injections into the granule cell layer, ventrolateral thalamus and CbN, corroborate to suggest that the nucleocortical pathway is formed in part by collaterals of premotor output neurons of the CbN.

Genetically distinct CbN neurons branch to innervate red nucleus and granule cell layer

We next addressed whether CbN output neurons that target the red nucleus collateralize to the cerebellar cortex. To selectively label CbN-to-red nucleus neurons, we combined the use of a Cre-driver mouse line expressing Cre in the CbN and a Cre-dependent viral tracer. This technique mitigated a potential confound with conventional tracer injections into the red nucleus, since the red nucleus projects directly to the cerebellum (Dietrichs, 1983; Huisman et al., 1983); the viral tracer would be expected to only express the reporter protein in cerebellar nuclear axons.

In Ntsr1-Cre x Rosa26-tdTomato mice, somatic Cre expression is evident in the cerebellar nuclei but not in the red nucleus (Fig 3A). Following injections of the Cre-dependent virus retrogradely transported virus AAV1.Flex.eGFP (Rothermel et al., 2013) into the red nucleus of Ntsr1-Cre mice (Fig. 3B,C,D; n=4 mice), we observed GFP-labeled terminals at the injection site, indicating successful uptake and expression of the virus (Fig. 3D). These injections retrogradely labeled somata in anterior and posterior regions of the contralateral interposed nucleus(Fig. 2J; 3E) and in all cases putative collateral axons continued to course up to and terminate as mossy fiber rosettes in the granule cell layer of the 4/5 and Simple lobules (Fig. 2I; 3E,F; n=5 injections). In addition, viral injections into the red nucleus also labeled large boutons in the ventrolateral thalamus, which were indistinguishable in morphology from those seen following BDA injections into the granule cell layer, CbN or red nucleus (Fig. 2L; 3G), consistent with the idea that a population of CbN output neurons branch to innervate the red nucleus, ventrolateral thalamus and cerebellar cortex.

In some instances, sparse somatic label was observed in Cre-expressing areas adjacent to the red nucleus injection site, specifically the mesencephalic reticular formation (n=4/5 injections), substantia nigra pars reticulata (n=3/5 injections) and the ventral tegmental area (n=3/5 injections). Notably, these regions are contiguous with the injection sites suggesting that somatic label could be a consequence of direct viral uptake by neighboring areas. Because these structures are not precerebellar, mossy fibers labeled in the cerebellar cortex are most likely to have originated from collaterals of CbN output neurons. Additionally, no retrograde label was observed in the cerebral cortex suggesting the corticorubral pathway, another main afferent to the red nucleus, does not express Cre. In conclusion, these data provide an anatomical route for copies of motor information sent to the red nucleus to reach the cerebellar cortex.

Nucleocortical mossy fiber terminal morphology

To facilitate comparisons of the nucleocortical mossy fiber pathway to extracerebellar mossy fibers, we next characterized their morphology. Close examination of the morphology of nucleocortical terminals in the cerebellar cortex revealed mossy fiber rosettes with a large, elongated central bulb surrounded by numerous small excrescences (1.5 to 5.5 μm in length), similar to mossy fibers from extracerebellar sources (Brodal and Drablos, 1963;

Palay and Chan-Palay, 1974). In many cases mossy fiber rosettes formed *en passant*, with axons continuing on to form secondary mossy fibers or filopodial endings. Comparing mossy fibers labeled by ventrolateral thalamus or red nucleus injections revealed indistinguishable morphology: following thalamic BDA injections, mossy fibers extended approximately 15 μm along the long axis and 8 μm across; following viral red nucleus injections, the fiber extended 16 μm by 9 μm across (BDA injections: long-axis range: 8.11 to 25.0 μm, mean±sem: 15.62 ± 1.06; short-axis range: 5.33 to 12.67 μm; mean±sem: 8.29 ± 0.4; n=22 terminals in 3 mice; viral injections: long-axis range: 9.32 to 24.42 μm; mean ±sem: 16.0 ± 0.78 μm long; short-axis range 4.65 to 12.68 μm mean±sem: 9.14 ± 0.37 μm wide; n=30 terminals in 3 mice; not significantly different p=0.77 for length, p= 0.13 for width, two-tailed t-test). These data indicate that nucleocortical output neurons targeting diverse structures form collateral mossy fibers with similar morphology in cerebellar cortex.

Mapping the nucleocortical collateral pathway

Previous studies of the nucleocortical pathway mapped it based on cerebellar cortical or cerebellar nuclear injections. Such experiments necessarily include the diverse types of nucleocortical axons including potential glycinergic and GABAergic components (Chan-Palay et al., 1979; Hámori and Takács, 1989; Batini et al., 1992; Uusisaari and Knöpfel, 2010). Our experiments allowed us to isolate and map the specific subset of the nucleocortical pathway comprised of collateral branches of premotor output neurons (Fig. 4). In a representative specimen, VL61213-1, injections of BDA to the ventrolateral thalamus labeled somata in all three cerebellar nuclei, consistent with previous reports (Angaut et al., 1968, 1986; Angaut and Bowsher, 1970; Kalil, 1981). Specifically, somata were localized to the middle sections of the dentate, caudal regions of the anterior interposed, throughout the posterior interposed and caudal-most regions of the fastigial nuclei. In this specimen, putative nucleocortical mossy fibers were most densely clustered in the granule cell layer of lobules 4/5, Crus I, Crus II and paramedian, with additional rosettes found in cerebellar lobules 3, 6, 7, 8/9, 10, Simple and copula pyramis (Fig. 4A). Across specimen, retrograde label in the CbN following ventrolateral thalamus injections was most dense contralateral to the injection site, but weak ipsilateral label was also seen in 9/11 cases, suggesting both crossed and uncrossed pathways from the cerebellum (Chan-Palay, 1977; Faull and Carman, 1978; Teune et al., 2000; Gonzalez-Joekes and Schreurs, 2012; Ruigrok and Teune, 2014). Additionally, retrograde label was usually observed in all three of the cerebellar nuclei (n=9/11). Within the granule cell layer, ventrolateral thalamus injections labeled mossy fibers concentrated in the Simple, Crus I and Crus II lobules. Smaller numbers of terminals were found across animals in lobules 3, 4/5, 6, 7, 8/9, 10, paraflocculus, paramedian and copula pyramis.

Cre-dependent viral injections into the red nucleus of Ntsr1-Cre mice labeled neurons restricted to the contralateral anterior and posterior interposed nuclei in all cases (n=5/5 injections). In a representative animal, RN91714-3, nucleocortical terminals were confined to lobules 3, 4/5, Crus II, Simple, Paramedian and Cop of the granule cell layer (Fig. 4B). Across specimen, most terminals appeared in lobules 4/5 and Simple (Fig. 4C), with fewer terminals labeled in the cerebellar lobules 3, Crus I, Crus II, paramedian and copula pyramis. In contrast to the restricted retrograde GFP expression with the interposed nuclei,

BDA injections into the RN retrogradely labeled all three cerebellar nuclei in some cases (n=6/9 mice), only two nuclei in other cases (n=2/9) and one labeled somata solely in the anterior and posterior regions of the interposed nucleus, suggesting potential uptake by fibers-of-passage, including axons coursing toward the ventrolateral thalamus but not terminating in the red nucleus. These data are in agreement with previous studies showing cerebellar projections to the red nucleus originate from the interposed nucleus (McCrea et al., 1978; Daniel et al., 1987; Shinoda et al., 1988).

The nucleocortical pathway terminates in the putative delay eyelid conditioning microzone

Recent studies have identified a region of the cerebellar cortex at the base of the primary fissure between 4/5 and Simple lobules as being involved in the generation of eyelid closures during delay eyelid conditioning, and have termed it the “eyelid conditioning microzone” (Heiney et al., 2014; Steinmetz and Freeman, 2014). The widespread distribution of nucleocortical terminals resulting from our BDA injections to the ventrolateral thalamus described above included this eyelid conditioning microzone near the primary fissure (2/11 cases). We therefore targeted this area directly to test if the nucleocortical pathway provides a source of feedback through collaterals of output neurons from the interposed nucleus. BDA injections into this region of the granule cell layer labeled somata in the rostral regions of anterior interposed nucleus and terminals in both the contralateral ventrolateral thalamus and red nucleus (Fig. 5; n=4 mice). The distribution of terminals in the red nucleus and ventrolateral thalamus following these injections was indistinguishable from that seen following injections into more posterior regions of the granule cell layer ranging in medial-lateral extent from the base at the primary fissure to the base joining the Simple and Crus I lobules. However, we did note that anterior delay eyelid conditioning zonal injections labeled approximately 60% fewer somata in both anterior and posterior cerebellar nuclei than the more posterior granule cell layer targets. Nevertheless, these data show that among the targets of the nucleocortical collateral pathway is a microzone involved in generating motor commands for conditioned eyelid closure.

Postsynaptic targets of nucleocortical collateral terminals

To evaluate whether nucleocortical mossy fiber rosettes likely form synapses, we stained the tissue with an antibody against SV2 assessing whether they contain synaptic vesicles. Mossy fiber rosettes labeled with either BDA or GFP were consistently immuno-positive for SV2 (Fig. 6A,D), suggesting that they likely contain synaptic vesicles (n=7 mice). SV2 immuno-positive boutons were also seen in the red nucleus and ventrolateral thalamus following BDA injections to the granule cell layer, suggesting that the collaterals there also form synapses (Fig. 6B,C,E).

To determine the cellular targets of nucleocortical mossy fibers, we combined collateral tracing from ventrolateral thalamus and red nucleus injections with immunostaining or electron microscopy to identify postsynaptic partners. Because nucleocortical mossy fibers targeted the granule layer, we focused on its two dominant cell types, Golgi cells and granule cells, as potential targets of these axons. We identified Golgi cells by using GlyT2-GFP mice or staining for mGluR2 or neurogranin, which together label the entire Golgi cell population (Simat et al., 2007). BDA injected into the ventrolateral thalamus (n=4) of

GlyT2-GFP mice labeled mossy fibers that expressed SV2 at interfaces with GFP-positive neurites in the granule cell layer (Fig. 7C). Mossy fibers from these injections also formed SV2 positive close contacts with mGluR2/3 immuno-positive neurites (n=4; Fig. 7B), as well as neurogranin immune-positive Golgi somata (n=3 with SV2 staining, n=7 total; Fig. 7A). Labeled mossy fibers from viral injections into Ntsr1-cre mice also made SV2+ close contacts with both mGluR2/3 immuno-positive neurites (n=4; Fig. 7E) and neurogranin-positive somata (n=4; Fig. 7D). Together these data suggest that the mossy fiber collateral terminals of the nucleocortical pathway make putative synapses onto Golgi cells of the cerebellar cortex, which could mediate feedforward inhibition onto downstream targets of Golgi cells, such as granule cells.

To our knowledge, granule cells lack immunohistochemical markers that clearly delineate their dendrites. Therefore, we used electron microscopy to determine if the mossy fiber terminals of collateralizing output neurons make synapses onto granule cells. We specifically examined mossy fiber terminals labeled with AAV1.Flex.eGFP injections into the red nucleus of Ntsr1-Cre mice. In comparisons with granule cell electron microscopic profiles of earlier studies, granule cell dendrites were identified based on their small caliber and position within the glomerulus (Palay and Chan-Palay, 1974). Such analysis also permitted identification of granule cells via their characteristic club-like dendrites. Labeled mossy fiber rosettes characteristically formed many lobes and inlets enveloping cross sections of granule cell dendrites with mitochondria (Fig. 8).

DAB-labeled, GFP-positive mossy fibers were visualized across sections as containing dense clusters of vesicles throughout and forming several lobes which encompassed anywhere from one to six granule cell dendrites in a 50 nm section. We found labeled mossy fibers containing vesicles apposed to post-synaptic densities on profiles characteristic of granule cell dendrites (Fig. 8; n=2 mice; Palay and Chan-Palay, 1974). Taken together, these data suggest that nuclear output neurons contact both Golgi and granule cells via collateral branches that form mossy fibers.

Discussion

The ability to make rapid, precise movements is mediated by the cerebellum. Prominent theories propose that the cerebellum utilizes internal feedback for real-time modifications of movement trajectories, since sensory reafference can be slow relative to motor commands (Wolpert et al., 1998; Franklin and Wolpert, 2011). Corollary discharge, defined here as a copy of a motor command sent away from the muscles (Sommer and Wurtz, 2008), is integral to internal model computations thought to be made by the cerebellum. Thus, identifying sources of corollary discharge information to the cerebellum is a critical step toward mechanistically testing this hypothesis. In the present study, we show that projection neurons of the cerebellar nuclei branch to form mossy fibers in the granule cell layer, constituting part of the nucleocortical pathway. These findings provide a candidate pathway for future research investigating the role of corollary discharge in cerebellar function.

Prior research on the nucleocortical pathway suggested that it was in part composed of collaterals of output neurons, but the experimental evidence underlying this view was

indirect: First, collision experiments in which CbN neurons were recorded during stimulation of the cerebellar cortex and/or ventrolateral thalamus suggested that the same cells project to both targets (Tolbert et al., 1976, 1977, 1978; McCrea et al., 1978). Horseradish peroxidase fills of single CbN neurons recorded intracellularly also pointed to collateralization of nuclear output neurons, but complete reconstructions were not possible, leaving the targets unclear (McCrea et al., 1978). Finally, using dual label techniques, a small number of CbN neurons co-labeled after cerebellar cortex tracer injections and ventrolateral thalamus injections (Payne, 1983). Most studies examining the nucleocortical pathway used tracing from injections into either the cerebellar cortex or nuclei, making it impossible to differentiate between the contribution of nucleocortical fibers from CbN premotor output neurons and other cell types (Gould and Graybiel, 1976; Tolbert et al., 1976, 1980; Dietrichs and Walberg, 1979, 1980). Indeed, a recent report demonstrating glycinergic nucleocortical projections in brain slices highlights the importance of isolating subpopulations of nucleocortical projections in mice since the nucleocortical population is diverse (Uusisaari and Knöpfel, 2010).

The nucleocortical collateral pathway

Our work provides anatomical evidence that cerebellar neurons collateralize to innervate the granule layer, and directly demonstrates that the CbN neurons innervating premotor structures such as red nucleus and ventrolateral thalamus collateralize to the granule cell layer where they contact granule and Golgi cells. By labeling branches of nuclear output neurons with BDA injections into the ventrolateral thalamus or AAV1.Flex.eGFP into the red nucleus of Ntsr1-Cre mice, we were able to exclusively map the collateral pathway of the nucleocortical tract. These axons terminate as mossy fibers in the granule cell layer, where they contacted Golgi and granule cells (Figs. 1, 2). Our studies do not address whether nucleocortical mossy fibers are molecularly distinct from mossy fibers originating from precerebellar sources. Precedent for molecularly diverse mossy fibers exists, however, raising the question of whether nucleocortical mossy fibers may be molecularly distinct from other mossy fibers (Sillitoe et al., 2003; Gebre et al., 2011).

The majority of nucleocortical collateral axons were found to target cortical regions of the $4^{th}/5^{th}$ lobule shown to receive sensory input from hind and forelimbs in both rats and cats (Provini et al., 1968; Buisseret-Delmas and Angaut, 1993), and the Crus I lobule thought to receive sensory and motor input from the face and vibrissa of mice (Proville et al., 2014). In addition, we located nucleocortical collateral axons targeting a more anterior cortical zone that has been recently identified to participate in eyelid conditioning (Heiney et al., 2014; Steinmetz and Freeman, 2014). Nucleocortical innervation of the eyelid conditioning microzone in Crus I suggests a potential source of corollary discharge information in conditioning circuitry. This finding is of note because comparisons of vestibular ocular reflex (VOR) and eyelid conditioning circuitry highlight an apparent and anomalous lack of corollary discharge in eyelid conditioning circuitry (Raymond et al., 1996). Our data suggest a potential corollary discharge pathway within eyelid conditioning circuitry, resolving the anomalous understanding of eyelid conditioning circuitry that was notable given the general uniformity of cerebellar circuitry. VOR circuitry is proposed to receive corollary discharge information from the prepositus hypoglossus brainstem nucleus reporting eye movement

commands to the cerebellar cortex and extraocular motor neurons (Stone and Lisberger, 1990; Green et al., 2007; Lisberger, 2009). The nucleocortical pathway is an excellent candidate to reconcile the difference between smooth pursuit and eyelid conditioning since in part originates in the interposed cerebellar nucleus critical to eyelid conditioning and terminates in areas recently shown to control eyelid closure in mice (Heiney et al., 2014; Steinmetz and Freeman, 2014). This anatomical arrangement suggests that conditioned responses driven by elevated CbN output would be communicated to the cerebellar cortex and might interact with mossy fiber pathways communicating the conditioning stimulus at the level of the granule cell layer.

Anatomy of CbN outputs

The present data provided further support for collateralization of cerebellar output neurons within the brainstem and midbrain. Labeling from our injections into the cerebellar cortex, CbN, red nucleus and ventrolateral thalamus was consistent, substantiating findings that some nuclear projection neurons branch to innervate multiple premotor target regions (Tolbert et al., 1976; McCrea et al., 1978; Shinoda et al., 1988; Teune et al., 1995; Ruigrok and Teune, 2014): BDA injections into the ventrolateral thalamus labeled terminals but not somata in the red nucleus and cerebellar cortex; BDA injections into the cerebellar cortex labeled somata in the CbN and terminal boutons in the red nucleus and ventrolateral thalamus; BDA injections into the CbN labeled boutons in the cerebellar cortex, red nucleus and ventrolateral thalamus. Complementary viral injections into the red nucleus of Ntsr1-Cre mice resulted in GFP labeled terminals and not somata in the ventrolateral thalamus and granule cell layer. Together, this suite of data is consistent with collateralization of nuclear output neurons that supply outgoing command information to a minimum of three locations – cerebellar cortex, red nucleus, and ventrolateral thalamus.

Additionally, our data are consistent with literature across species reporting that projections to the ventrolateral thalamus originate in all cerebellar nuclei - fastigial, interposed and dentate (Angaut et al., 1968, 1986; Angaut and Bowsher, 1970; Kalil, 1981). The fact that all three nuclei contained retrogradely labeled neurons following ventrolateral thalamus injections could explain the wide distribution of mossy fibers in the cerebellar cortex, which are believed to be topographically organized in other species (Haines and Pearson, 1979; Haines, 1989; Päällysaho et al., 1990; Trott et al., 1990). Indeed, granule cell layer injections between Simple and 6 lobules retrogradely labeled somata only in the interposed nucleus suggesting that topographic organization of the nucleocortical pathway in mice is conserved (Gould and Graybiel, 1976; Tolbert et al., 1976; Dietrichs and Walberg, 1979, 1980; Houck and Person, 2013). Similar to previous studies suggesting that cerebellar projections to the red nucleus are localized to the interposed nucleus (Daniel et al., 1987; Teune et al., 2000), our results from viral injections to the red nucleus suggest only a subset of output neurons from the interposed branch to innervate the red nucleus.

Targets of nucleocortical collaterals

Corollary discharge information is predicted to enhance or inhibit convergent sensory streams. Therefore, understanding the targets of the pathway could provide anatomical substrates for these types of interactions. For example, convergence of excitatory corollary

discharge and sensory feedback on granule cells could summate and enhance information transfer. Alternatively, corollary discharge could inhibit convergent sensory input by recruiting Golgi cells (Sperry, 1950; Bell, 1981; Guthrie et al., 1983; Bell and Grant, 1989; Mohr et al., 2003; Bellebaum et al., 2005; Bell et al., 2008; Crapse and Sommer, 2008; Huang et al., 2013). Anatomical evidence for both targets was revealed by our experiments. While previous electron microscopy (EM) studies of the nucleocortical pathway (Tolbert et al., 1980) relied on tracer injections directly into the CbN, potentially labeling a variety of nucleocortical axon types, our experiments restricted EM analysis to collateral branches. Using viral injections into the red nucleus of Ntsr1-Cre mice, we restricted electron-dense mossy fiber label to only bifurcating axons of CbN output neurons and identified mossy fiber synapses onto granule cells. At the EM level, labeled terminals in the granule cell layer possessed vesicles apposed to postsynaptic densities onto putative granule cell dendrites (Fig. 8). In addition, at the light microscope level, we found many contacts between nucleocortical collateral branches and Golgi cells labeled with a variety of markers, including GlyT2-GFP, neurogranin and mGluR2/3.

Together these results suggest that nucleocortical collateral branches could shape convergent inputs into the cerebellum via summation at granule cells directly or through inhibition of convergent inputs via Golgi cell-mediated inhibition.

The nucleocortical collateral tract as a corollary discharge pathway

Classifying the nucleocortical collateral pathway as a corollary discharge circuit is predicated on an anatomical criterion put forth by Sommer and Wurtz (2008). Their framework defines a corollary discharge pathway as originating in an area involved in generating movement, but traveling away from the muscles. Activity in the CbN can drive short latency movements following optogenetic silencing of Purkinje neurons (Heiney et al., 2014), and cerebellar-dependent conditioned eyelid closures can be learned and produced by the cerebellum alone in decerebrate animals (Hesslow, 1994). Therefore, the CbN can be considered an area involved in producing movement, and the nucleocortical collateral pathway projects away from the muscles relative to the output branches innervating the red nucleus. Thus, the nucleocortical collateral pathway appears to satisfy the anatomical criterion to be defined as a corollary discharge pathway.

In conclusion, our experimental results provide a means by which feedback of cerebellar commands could modify incoming sensory information at the level of the granule cell. Because this subdivision of the nucleocortical pathway provides a type of corollary discharge to synaptic targets almost immediately, it is an ideal mechanism for executing adjustments of ongoing cerebellar commands enabling precise movements.

Acknowledgments

We thank Dr. Jennifer Bourne for expert help with electron microscope tissue preparation and imaging. Work was supported by NIH R01 NS084996-01, Klingenstein Foundation Award in the Neurosciences, and Alfred P Sloan Foundation Fellowship to ALP, a Boettcher Investigator. Light microscopic experiments were performed in the University of Colorado Anschutz Medical Campus Advance Light Microscopy Core supported in part by Rocky Mountain Neurological Disorders Core Grant Number P30NS048154 and by NIH/NCRR Colorado CTSI Grant Number UL1 RR025780. We also thank the Electron Microscopy Center at the University of Colorado Anschutz Medical Campus for EM resources.

Literature Cited

Angaut P, Batini C, Billard JM, Daniel H. The cerebellorubral projection in the rat: retrograde anatomical study. Neurosci Lett. 1986; 68:63–68. [PubMed: 3014399]

Angaut P, Bowsher D. Ascending projections of the medial cerebellar (fastigial) nucleus: an experimental study in the cat. Brain Res. 1970; 24:49–68. [PubMed: 5503234]

Angaut P, Compoint C, Buisseret-Delmas C, Batini C. Synaptic connections of Purkinje cell axons with nucleocortical neurones in the cerebellar medial nucleus of the rat. Neurosci Res. 1996; 26:345–348. [PubMed: 9004272]

Angaut P, Guilbaud G, Reymond MC. An electrophysiological study of the cerebellar projections to the nucleus ventralis lateralis of thalamus in the cat. I. Nuclei fastigii et inerpositus. J Comp Neurol. 1968; 134:9–20. [PubMed: 5712414]

Batini C, Compoint C, Buisseret-Delmas C, Daniel H, Guegan M. Cerebellar nuclei and the nucleocortical projections in the rat: retrograde tracing coupled to GABA and glutamate immunohistochemistry. J Comp Neurol. 1992; 315:74–84. [PubMed: 1371781]

Bell CC. An efference copy which is modified by reafferent input. Science. 1981; 214:450–453. [PubMed: 7291985]

Bell CC, Grant K. Corollary discharge inhibition and preservation of temporal information in a sensory nucleus of mormyrid electric fish. J Neurosci Off J Soc Neurosci. 1989; 9:1029–1044.

Bell CC, Han V, Sawtell NB. Cerebellum-like structures and their implications for cerebellar function. Annu Rev Neurosci. 2008; 31:1–24. [PubMed: 18275284]

Bellebaum C, Daum I, Koch B, Schwarz M, Hoffmann K-P. The role of the human thalamus in processing corollary discharge. Brain J Neurol. 2005; 128:1139–1154.

Brodal A, Drablos PA. Two types of mossy fiber terminals in the cerebellum and their regional distribution. J Comp Neurol. 1963; 121:173–187. [PubMed: 14066521]

Buckley K, Kelly RB. Identification of a transmembrane glycoprotein specific for secretory vesicles of neural and endocrine cells. J Cell Biol. 1985; 100:1284–1294. [PubMed: 2579958]

Buisseret-Delmas C, Angaut P. The cerebellar olivo-corticonuclear connections in the rat. Prog Neurobiol. 1993; 40:63–87. [PubMed: 8424128]

Chan-Palay, V. Cerebellar Dentate Nucleus: Organization, Cytology and Transmitters. Springer-Verlag; 1977.

Chan-Palay V, Palay SL, Wu JY. Gamma-aminobutyric acid pathways in the cerebellum studied by retrograde and anterograde transport of glutamic acid decarboxylase antibody after in vivo injections. Anat Embryol (Berl). 1979; 157:1–14. [PubMed: 92901]

Clarke PG. Some visual and other connections to the cerebellum of the pigeon. J Comp Neurol. 1977; 174:535–552. [PubMed: 903417]

Crapse TB, Sommer MA. Corollary discharge across the animal kingdom. Nat Rev Neurosci. 2008; 9:587–600. [PubMed: 18641666]

Daniel H, Billard JM, Angaut P, Batini C. The interposito-rubrospinal system. Anatomical tracing of a motor control pathway in the rat. Neurosci Res. 1987; 5:87–112. [PubMed: 3431757]

Dietrichs E. The cerebellar corticonuclear and nucleocortical projections in the cat as studied with anterograde and retrograde transport of horseradish peroxidase. V. The posterior lobe vermis and the flocculo-nodular lobe. Anat Embryol (Berl). 1983; 167:449–462. [PubMed: 6625198]

Dietrichs E, Walberg F. The cerebellar corticonuclear and nucleocortical projections in the cat as studied with anterograde and retrograde transport of horseradish peroxidase. I. The paramedian lobule. Anat Embryol (Berl). 1979; 158:13–39. [PubMed: 93421]

Dietrichs E, Walberg F. The cerebellar corticonuclear and nucleocortical projections in the cat as studied with anterograde and retrograde transport of horseradish peroxidase. II. Lobulus simplex, crus I and II. Anat Embryol (Berl). 1980; 161:83–103. [PubMed: 6160791]

Faull RL, Carman JB. The cerebellofugal projections in the brachium conjunctivum of the rat I. The contralateral ascending pathway. J Comp Neurol. 1978; 178:495–517. [PubMed: 19626723]

Franklin DW, Wolpert DM. Computational mechanisms of sensorimotor control. Neuron. 2011; 72:425–442. [PubMed: 22078503]

Fu Y, Tvrdik P, Makki N, Paxinos G, Watson C. Precerebellar cell groups in the hindbrain of the mouse defined by retrograde tracing and correlated with cumulative Wnt1-cre genetic labeling. Cerebellum Lond Engl. 2011; 10:570–584.

Gebre SA, Reeber SL, Sillitoe RV. Parasagittal compartmentation of cerebellar mossy fibers as revealed by the patterned expression of vesicular glutamate transporters VGLUT1 and VGLUT2. Brain Structure and Function. 2012; 217(2):165–180. [PubMed: 21814870]

Gonzalez-Joekes J, Schreurs BG. Anatomical characterization of a rabbit cerebellar eyeblink premotor pathway using pseudorabies and identification of a local modulatory network in anterior interpositus. J Neurosci Off J Soc Neurosci. 2012; 32:12472–12487.

Gould BB, Graybiel AM. Afferents to the cerebellar cortex in the cat: evidence for an intrinsic pathway leading from the deep nuclei to the cortex. Brain Res. 1976; 110:601–611. [PubMed: 947474]

Green AM, Meng H, Angelaki DE. A reevaluation of the inverse dynamic model for eye movements. J Neurosci Off J Soc Neurosci. 2007; 27:1346–1355.

Guthrie BL, Porter JD, Sparks DL. Corollary discharge provides accurate eye position information to the oculomotor system. Science. 1983; 221:1193–1195. [PubMed: 6612334]

Haines DE. HRP study of cerebellar corticonuclear-nucleocortical topography of the dorsal culminate lobule--lobule V--in a prosimian primate (Galago): with comments on nucleocortical cell types. J Comp Neurol. 1989; 282:274–292. [PubMed: 2468700]

Haines DE, Pearson JC. Cerebellar corticonuclear - nucleocortical topography: a study of the tree shrew (Tupaia) paraflocculus. J Comp Neurol. 1979; 187:745–758. [PubMed: 90685]

Hámori J, Takács J. Two types of GABA-containing axon terminals in cerebellar glomeruli of cat: an immunogold-EM study. Exp Brain Res. 1989; 74:471–479. [PubMed: 2707323]

Harris KM, Perry E, Bourne J, Feinberg M, Ostroff L, Hurlburt J. Uniform serial sectioning for transmission electron microscopy. J Neurosci Off J Soc Neurosci. 2006; 26:12101–12103.

Heiney SA, Kim J, Augustine GJ, Medina JF. Precise control of movement kinematics by optogenetic inhibition of Purkinje cell activity. J Neurosci Off J Soc Neurosci. 2014; 34:2321–2330.

Hendelman WJ, Marshall KC. Axonal projection patterns visualized with horseradish peroxidase in organized cultures of cerebellum. Neuroscience. 1980; 5:1833–1846. [PubMed: 7432625]

Hesslow G. Inhibition of classically conditioned eyeblink responses by stimulation of the cerebellar cortex in the decerebrate cat. J Physiol. 1994; 476:245–256. [PubMed: 8046641]

Houck BD, Person AL. Cerebellar Loops: A Review of the Nucleocortical Pathway. Cerebellum Lond Engl. 2013

Huang C-C, Sugino K, Shima Y, Guo C, Bai S, Mensh BD, Nelson SB, Hantman AW. Convergence of pontine and proprioceptive streams onto multimodal cerebellar granule cells. eLife. 2013; 2:e00400. [PubMed: 23467508]

Huisman AM, Kuypers HG, Ververs B. Retrograde neuronal labeling of cells of origin of descending brainstem pathways in rat using SITS as a retrograde tracer. Brain Res. 1983; 289:305–310. [PubMed: 6661648]

Husson Z, Rousseau CV, Broll I, Zeilhofer HU, Dieudonné S. Differential GABAergic and glycinergic inputs of inhibitory interneurons and purkinje cells to principal cells of the cerebellar nuclei. The Journal of Neuroscience. 2014; 34(28):9418–9431. [PubMed: 25009273]

Ito M. The modifiable neuronal network of the cerebellum. Jpn J Physiol. 1984; 34:781–792. [PubMed: 6099855]

Kalil K. Projections of the cerebellar and dorsal column nuclei upon the thalamus of the rhesus monkey. J Comp Neurol. 1981; 195:25–50. [PubMed: 7204651]

Kawato M, Gomi H. The cerebellum and VOR/OKR learning models. Trends Neurosci. 1992; 15:445–453. [PubMed: 1281352]

Kolston J, Apps R, Trott JR. A combined retrograde tracer and GABA-immunocytochemical study of the projection from nucleus interpositus posterior to the posterior lobe C2 zone of the cat cerebellum. Eur J Neurosci. 1995; 7:926–933. [PubMed: 7613628]

Lisberger SG. Internal models of eye movement in the floccular complex of the monkey cerebellum. Neuroscience. 2009; 162:763–776. [PubMed: 19336251]

Mauk MD, Thompson RF. Retention of classically conditioned eyelid responses following acute decerebration. Brain Res. 1987; 403:89–95. [PubMed: 3828818]

McCrea RA, Bishop GA, Kitai ST. Morphological and electrophysiological characteristics of projection neurons in the nucleus interpositus of the cat cerebellum. J Comp Neurol. 1978; 181:397–419. [PubMed: 690271]

Miall RC, Weir DJ, Wolpert DM, Stein JF. Is the cerebellum a smith predictor? J Mot Behav. 1993; 25:203–216. [PubMed: 12581990]

Mohr C, Roberts PD, Bell CC. The mormyromast region of the mormyrid electrosensory lobe. I. Responses to corollary discharge and electrosensory stimuli. J Neurophysiol. 2003; 90:1193–1210. [PubMed: 12904505]

Oberdick J, Sillitoe RV. Cerebellar zones: history, development, and function. The Cerebellum. 2011; 10(3):301–306. [PubMed: 21822545]

Ohyama T, Nores WL, Murphy M, Mauk MD. What the cerebellum computes. Trends Neurosci. 2003; 26:222–227. [PubMed: 12689774]

Päällysaho J, Sugita S, Noda H. Cerebellar corticonuclear and nucleocortical projections in the vermis of posterior lobe of the rat as studied with anterograde and retrograde transport of WGA-HRP. Neurosci Res. 1990; 8:158–178. [PubMed: 2170877]

Palay, SL.; Chan-Palay, V. Cerebellar Cortex: Cytology and Organization. Springer; Berlin Heidelberg: 1974.

Paxinos, G.; Franklin, KBJ. The Mouse Brain in Stereotaxic Coordinates. 3. Elsevier Academic Press; 2008.

Payne JN. The cerebellar nucleo-cortical projection in the rat studied by the retrograde fluorescent double-labelling method. Brain Res. 1983; 271:141–144. [PubMed: 6192877]

Proville RD, Spolidoro M, Guyon N, Dugué GP, Selimi F, Isope P, Popa D, Léna C. Cerebellum involvement in cortical sensorimotor circuits for the control of voluntary movements. Nat Neurosci. 2014; 17:1233–1239. [PubMed: 25064850]

Provini L, Redman S, Strata P. Mossy and climbing fibre organization on the anterior lobe of the cerebellum activated by forelimb and hindlimb areas of the sensorimotor cortex. Exp Brain Res. 1968; 6:216–233. [PubMed: 5712701]

Raymond JL, Lisberger SG, Mauk MD. The cerebellum: a neuronal learning machine? Science. 1996; 272:1126–1131. [PubMed: 8638157]

Rivlin PK, Raymond PA. Use of osmium tetroxide-potassium ferricyanide in reconstructing cells from serial ultrathin sections. J Neurosci Methods. 1987; 20:23–33. [PubMed: 2438519]

Rothermel M, Brunert D, Zabawa C, Díaz-Quesada M, Wachowiak M. Transgene expression in target-defined neuron populations mediated by retrograde infection with adeno-associated viral vectors. J Neurosci Off J Soc Neurosci. 2013; 33:15195–15206.

Ruigrok TJH, Teune TM. Collateralization of cerebellar output to functionally distinct brainstem areas. A retrograde, non-fluorescent tracing study in the rat. Front Syst Neurosci. 2014; 8:23. [PubMed: 24600356]

Shadmehr R, Krakauer JW. A computational neuroanatomy for motor control. Exp Brain Res. 2008; 185:359–381. [PubMed: 18251019]

Shinoda Y, Futami T, Mitoma H, Yokota J. Morphology of single neurones in the cerebello-rubrospinal system. Behav Brain Res. 1988; 28:59–64. [PubMed: 3382520]

Sillitoe RV, Benson MA, Blake DJ, Hawkes R. Abnormal dysbindin expression in cerebellar mossy fiber synapses in the mdx mouse model of Duchenne muscular dystrophy. J Neurosci. 2003; 23(16):6576–6585. [PubMed: 12878699]

Simat M, Parpan F, Fritschy J-M. Heterogeneity of glycinergic and gabaergic interneurons in the granule cell layer of mouse cerebellum. J Comp Neurol. 2007; 500:71–83. [PubMed: 17099896]

Sommer MA, Wurtz RH. Brain circuits for the internal monitoring of movements. Annu Rev Neurosci. 2008; 31:317–338. [PubMed: 18558858]

Sperry RW. Neural basis of the spontaneous optokinetic response produced by visual inversion. J Comp Physiol Psychol. 1950; 43:482–489. [PubMed: 14794830]

Steinmetz AB, Freeman JH. Localization of the cerebellar cortical zone mediating acquisition of eyeblink conditioning in rats. Neurobiol Learn Mem. 2014; 114C:148–154. [PubMed: 24931828]

Stone LS, Lisberger SG. Visual responses of Purkinje cells in the cerebellar flocculus during smooth-pursuit eye movements in monkeys. I. Simple spikes. J Neurophysiol. 1990; 63:1241–1261. [PubMed: 2358872]

Teune TM, van der Burg J, Ruigrok TJ. Cerebellar projections to the red nucleus and inferior olive originate from separate populations of neurons in the rat: a non-fluorescent double labeling study. Brain Res. 1995; 673:313–319. [PubMed: 7606446]

Teune TM, van der Burg J, van der Moer J, Voogd J, Ruigrok TJ. Topography of cerebellar nuclear projections to the brain stem in the rat. Prog Brain Res. 2000; 124:141–172. [PubMed: 10943123]

Tolbert D, Kultas-Ilinsky K, Ilinsky I. EM-autoradiography of cerebellar nucleocortical terminals in the cat. Anat Embryol (Berl). 1980; 161:215–223. [PubMed: 7469042]

Tolbert DL, Bantli H, Bloedel JR. Anatomical and physiological evidence for a cerebellar nucleo-cortical projection in the cat. Neuroscience. 1976; 1:205–217. [PubMed: 11370232]

Tolbert DL, Bantli H, Bloedel JR. The intracerebellar nucleocortical projection in a primate. Exp Brain Res. 1977; 30:425–434. [PubMed: 413728]

Tolbert DL, Bantli H, Bloedel JR. Multiple branching of cerebellar efferent projections in cats. Exp Brain Res. 1978; 31:305–316. [PubMed: 648599]

Trott JR, Apps R, Armstrong DM. Topographical organisation within the cerebellar nucleocortical projection to the paravermal cortex of lobule Vb/c in the cat. Exp Brain Res. 1990; 80:415–428. [PubMed: 1694139]

Uusisaari M, Knöpfel T. GlyT2+ neurons in the lateral cerebellar nucleus. Cerebellum Lond Engl. 2010; 9:42–55.

Wolpert DM. Computational approaches to motor control. Trends Cogn Sci. 1997; 1:209–216. [PubMed: 21223909]

Wolpert DM, Miall RC, Kawato M. Internal models in the cerebellum. Trends Cogn Sci. 1998; 2:338–347. [PubMed: 21227230]

Zeilhofer HU, Studler B, Arabadzisz D, Schweizer C, Ahmadi S, Layh B, Bösl MR, Fritschy J-M. Glycinergic neurons expressing enhanced green fluorescent protein in bacterial artificial chromosome transgenic mice. J Comp Neurol. 2005; 482:123–141. [PubMed: 15611994]

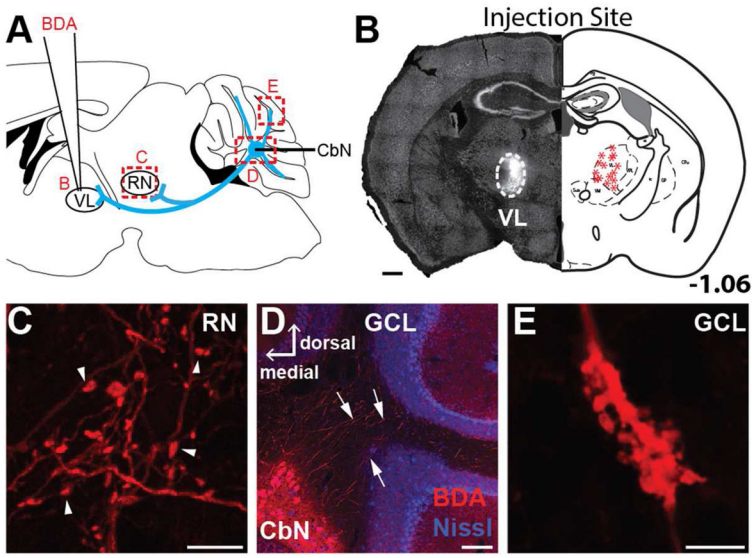

Figure 1.

Ventrolateral thalamus (VL) injections label terminals in the red nucleus (RN) and cerebellar cortex and somata in CbN (n=11). ***A.*** The schematic shows biotinylated dextran amine (BDA) injections into the VL. Based on predictions of bifurcating cerebellar nuclear (CbN) axons (blue), tissue from animals with BDA injections to the VL was analyzed for somatic label in the CbN and terminal label in the cerebellar cortex and RN(red boxes). ***B.*** An image of the VL injection site from a representative animal (left) is compared to the injections sites (asterisks) for all animals that received an injection to the VL in an atlas section of VL approximately 1.06 mm posterior to bregma (right). ***C.*** Putative terminals (arrowheads) were observed in the RN following VL injections. ***D.*** VL injections labeled somata in the CbN with putative collateral axons (arrows) extending to and terminating in the granule cell layer in section counterstained for Nissl. ***E.*** Mossy fiber rosette in lobule 4/5 of the granule cell layer following VL injection. Scales, B = 500 μm; C and E = 10 μm; D = 150 μm.

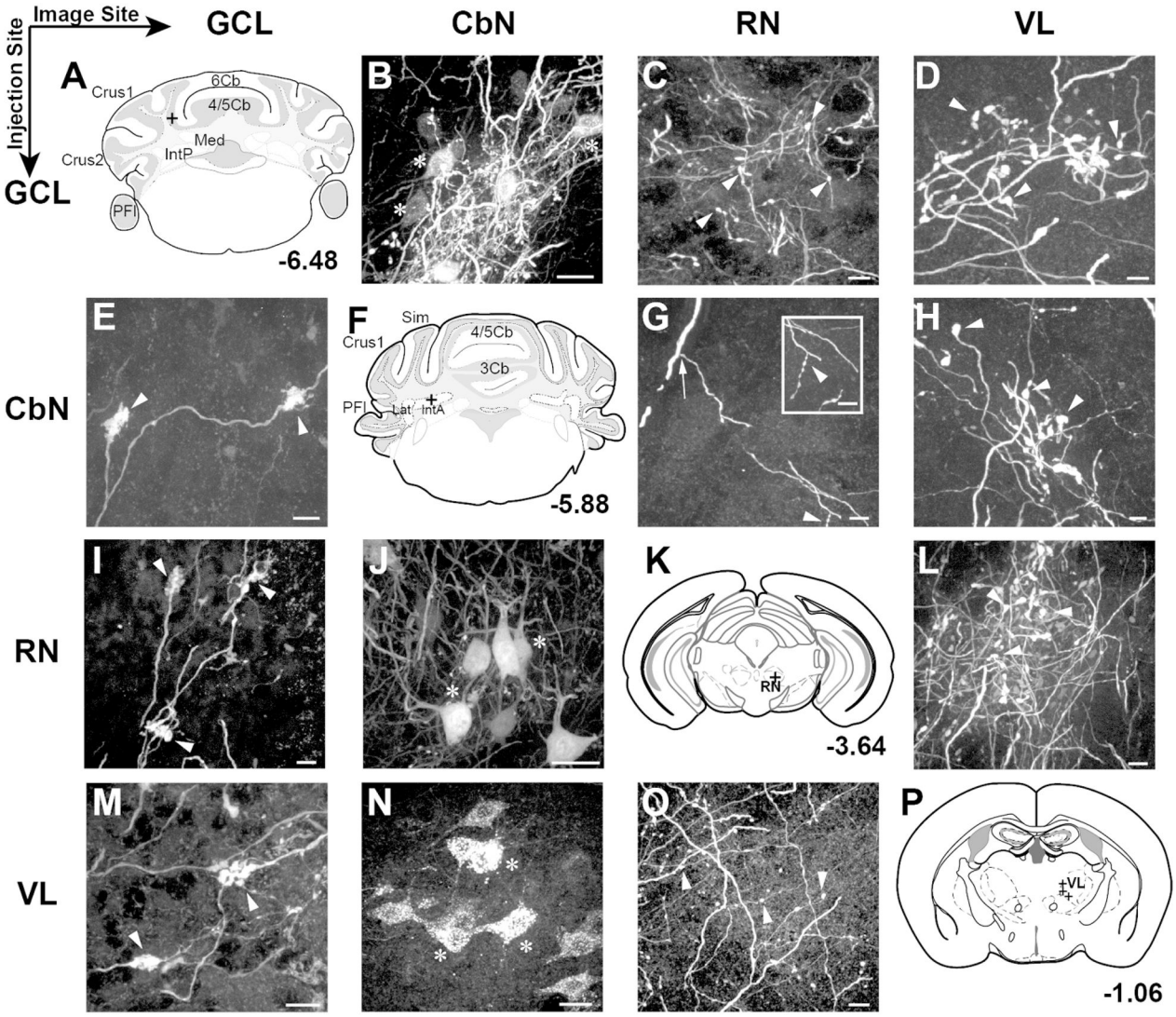

Figure 2.

Consistent structures were labeled along the course of CbN output neurons (columns) following BDA or viral injections into various sites along pathway (rows), including cerebellar cortex around the base of the Simple lobule, CbN, red nucleus (RN), and ventrolateral thalamus (VL). ***A–D:*** Row 1 shows somatic BDA label in the CbN (B), boutonal label in the RN (C) and boutonal label in the VL (D) following injections into the cerebellar cortex granule cell layer (sketched in A) (granule cell layer injection just posterior to Simple lobule, at the base between 4/5 and 6 lobule; n=5): ***E–H:*** Row 2 shows labeled mossy fiber rosettes in granule cell layer of 4/5 lobule (E); a sketch of the injection site (n=5) (F); labeled boutons in the RN (G) and labeled boutons in VL following injections into the anterior interposed nucleus (H). ***I–L*** Row 3 shows GFP expression in mossy fibers (I); GFP expression in somata of the interposed nucleus (J); a sketch of the injection site (K) and boutonal GFP expression in VL (L) following virus injections to the RN of Ntsr1-cre mice (n=5): ***M–P:*** Row 4 shows labeled mossy fibers (M); somata in anterior interposed

nucleus (N); terminal boutons in the RN (O) anda sketch of the injection site (P) following VL injection (n=11). Scales: B,J,N= 20 μm; C,D,E,G,H,I,L,M,O = 10 μm. Markers: Arrows, axons; Arrowheads, boutons; Asterisks, somata; Crosses, injection sites.

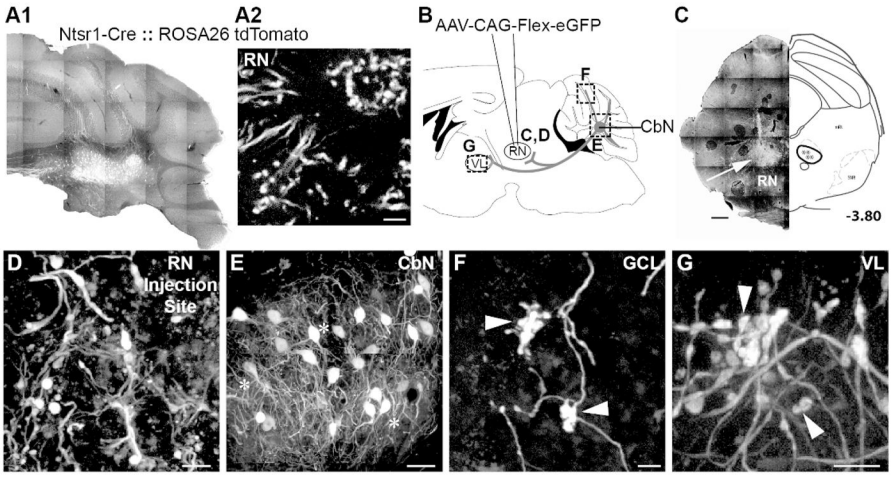

Figure 3.

Genetically identified cerebellar nuclear (CbN) neurons branch to innervate red nucleus (RN), ventrolateral thalamus (VL) and 3, 4/5, Simple, Crus I, Crus II, paramedian and copula pyramis lobules of the granule cell layer. ***A.*** Transgenic mice (Ntsr1-Cre::Rosa26-tdTomato) show Cre expression in CbN somata ***(A1)*** but not RN somata ***(A2). B.*** Schematic of AAV1-CAG-Flex-eGFP illustrates injections into the RN of Ntsr1-Cre mice. Tissue was analyzed for terminal label in the granule cell layer, somata label in the CbN and terminal label in the VL (dashed boxes) as well as elsewhere in midbrain and brainstem. ***C.*** RN injection site was marked by labeled terminal boutons after viral injections (left). An atlas section identifying RN approximately 3.80 mm posterior to bregma is included for context. Asterisks indicate injection sites for each animal (right). ***D.*** Higher magnification image of terminals in the rRN at the injection site confirm viral transfection of Cre-expressing axons, not RNsomata. ***E.*** Somata in the interposed nucleus express GFP following viral transfection of RN in Ntsr1-Cre mice. ***F.*** Mossy fiber rosettes in the granule cell layer (arrowheads) express GFP. ***G.*** Terminal boutons (arrowheads) in VL express GFP following RN viral injections. Scales: C = 500 μm; D, G = 20 μm; E = 50 μm; F = 10 μm.

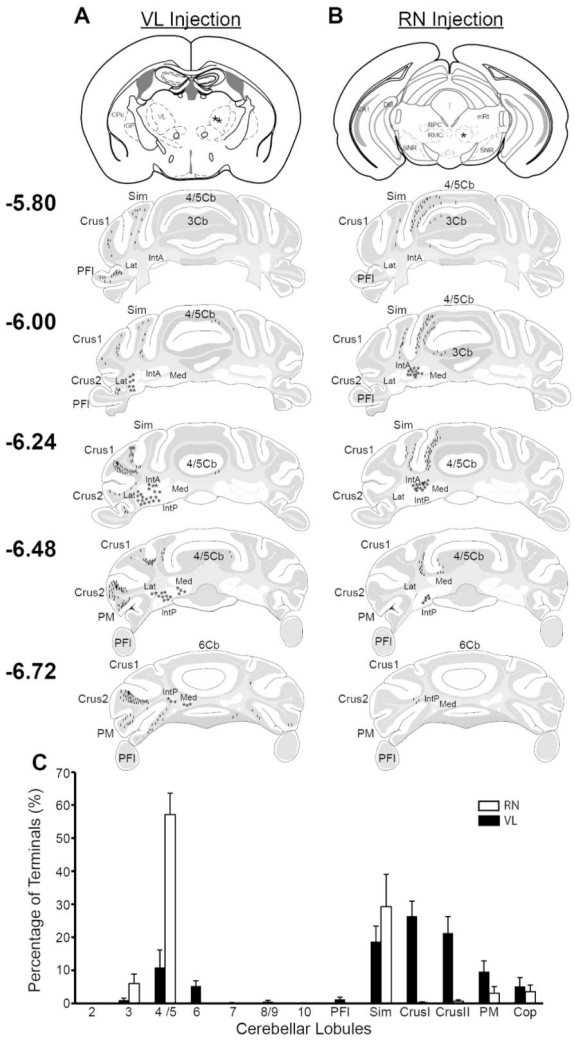

Figure 4.

Atlas sections showing location of nucleocortical collateral terminals labeled in the cerebellar cortex following ventrolateral (VL) and red nucleus (RN) injections which were then quantified. ***A. (top)*** Atlas section shows BDA injection site (asterisks) into VL. ***(lower)***Atlas sections show the location of terminals (tick marks) and somata (stars) following the injection shown above. ***B. (top)*** Atlas section shows viral injection site (asterisk) into the RN of an Ntsr1-cre mouse. ***(lower)*** Same convention as in A. ***C.*** The percentage of terminals counted in each cerebellar lobule was averaged across animals for VL (black bars; n=11) and RN (white bars; n=9) injections and plotted as mean ± sem. Abbrv: Cop - copula of the pyramis; PM - paramedian lobule; Crus I - crus 1 of the ansiform lobule; Crus II - crus 2 of the ansiform lobule; Sim - simple lobule; PFl – paraflocculus.

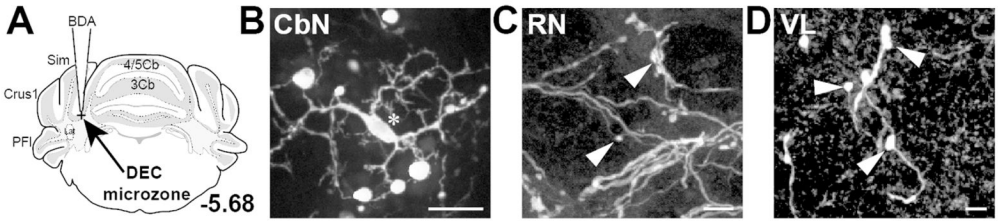

Figure 5.

CbN neurons produce putative collaterals targeting the “eyelid conditioning microzone” region of the cerebellar cortex, located at the apex of the primary fissure joining the Simple and 4/5 lobules (n=4 mice). ***A.*** An atlas section illustrates site of injection into eyelid conditioning zone of cerebellar cortex. ***B.*** BDA label in interposed nucleus somata was seen following injection into eyelid conditioning microzone. ***C.*** Terminal boutons in red nucleus (RN) were labeled with BDA following microzone injections; ***D.*** Terminal boutons in ventrolateral thalamus (VL) were labeled with BDA following microzone injections. Scales, B = 20 μm; C,D = 10 μm. Convention: Arrows, axons; Arrowheads, terminals; Asterisks, somata; Crosses, injection sites.

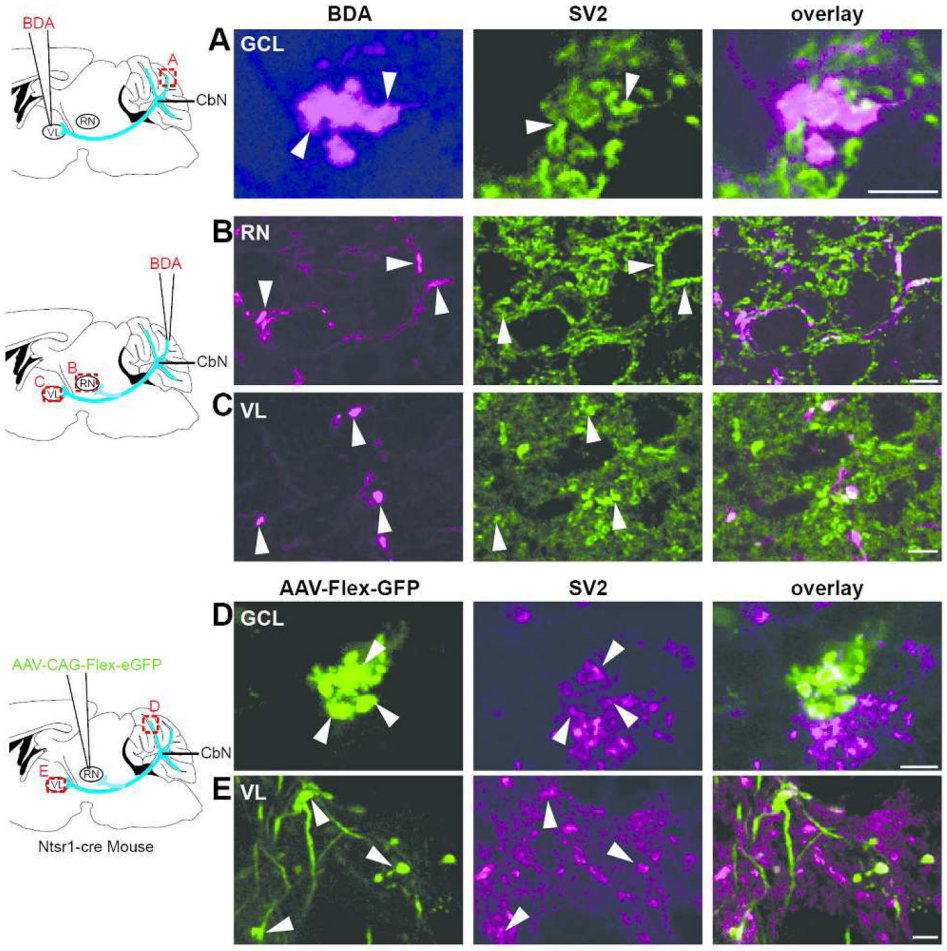

Figure 6.

BDA- and virally- labeled boutons are immunopositive for SV2. ***A. (far left)*** A schematic diagram illustrating site of BDA injection to the ventrolateral thalamus (VL) is shown; ***(left)*** A cerebellar mossy fiber rosette located in the Crus I lobule labeled with BDA after a VL injection was immunopositive for SV2 (***middle***) as shown in the overlay (***right***; n=3). Confocal stack thickness was 1.35 μm. ***B–C. (far left)*** Schematic diagram of site of BDA injections into the granule cell layer. (See text for the range of injection sites for these experiments.) ***(left)*** Terminal boutons labeled with BDA in the red nucleus (RN) after a granule cell layer injection at the base of the Simple lobule near the primary fissure (n=5) expressed SV2 ***(middle)*** as shown in the overlay ***(right)***. Confocal stack thickness was 1.7 μm. ***C. (left)*** BDA-labeled terminal boutons were observed in VL following granule cell layer injection at the base of the Simple lobule near the primary fissure (n=5); SV2 immunostaining ***(middle)*** overlayed with labeled terminal ***(right)***. Confocal stack thickness was 0.34 μm. ***D–E. D. (far left)*** A schematic of AAV1-CAG-Flex-eGFP injection into the red nucleus of Ntsr1-Cre mice is shown. ***(left)*** Terminal boutons labeled with GFP were observed in the granule cell layer of the 4/5 lobule following virus injections into the RN of Ntsr1-Cre mice (n=5); these terminals expressed SV2 ***(middle)*** as shown in overlay ***(right)***. Confocal stack thickness was 1.89 μm. ***E. (left)*** GFP-expressing terminal boutons were seen

in VL following viral injections to the RN of Ntsr1-Cre mice (n=5); SV2 immunostaining ***(middle)*** is overlayed with boutons ***(right)***. Confocal stack thickness was 1.62 μm. Scales, A,D = 5 μm; B,C and E = 10 μm.

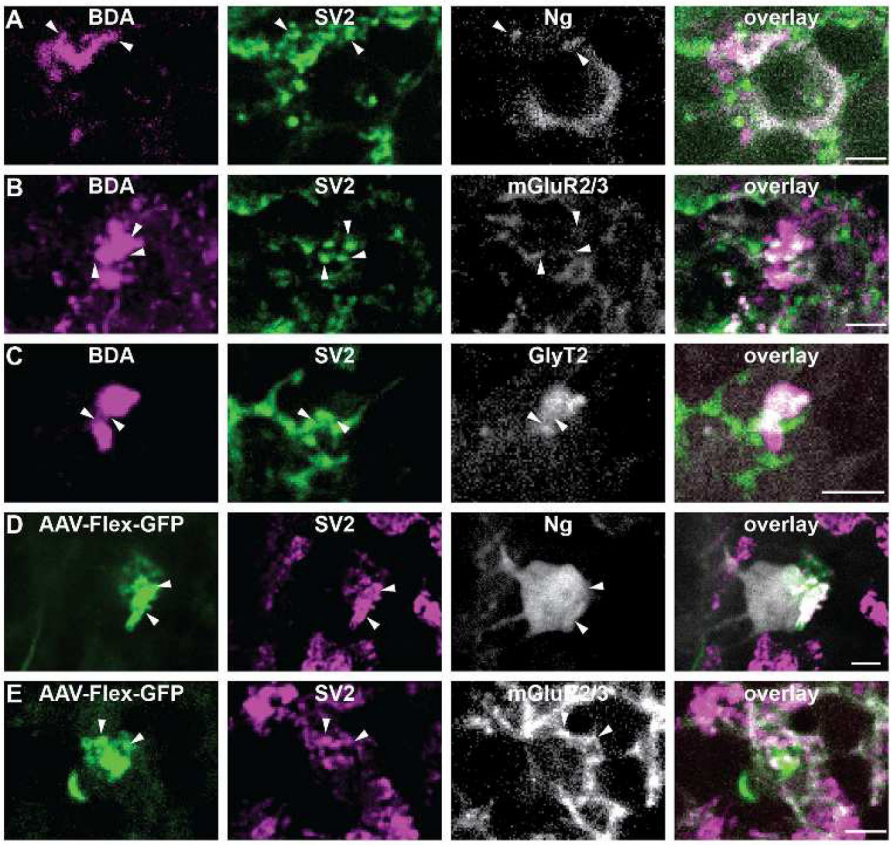

Figure 7.

Close contacts between nucleocortical terminals and Golgi cells were observed and express SV2. Each row follows a similar convention, showing terminal label at far left, followed by SV2 immunostaining, then Golgi cell markers and finally an overlay of the three signals. ***A.*** ***(far left)*** Nucleocortical mossy fiber bouton was labeled with ventrolateral thalamus BDA injection (n=3); ***(left middle)*** SV2 immunostaining colocalized with the labeled terminal; ***(right middle)*** neurogranin immunostaining was used to identify Golgi cells; ***(far right)*** an overlay of the channels illustrated SV2-expressing mossy fibers form close contacts with Golgi cell. Confocal stack thickness was 0.81μm. Arrowheads highlight sites of putative contacts onto Golgi cells. ***B.*** Conventions as in ***A*** but for mGluR2/3 immunostaining (n=3). Confocal stack thickness was 0.27μm. ***C.*** Conventions as in ***A*** but for glycinergic GFP-expressing Golgi cell (n=3). Confocal stack thickness was 2.16 μm. ***D.*** ***(far left)*** Conventions as in ***A*** but showing virally labeled nucleocortical mossy fiber. ***(left middle)*** (n=5) Confocal stack thickness was 2.16 μm. ***E.*** Conventions as in ***D*** but for mGluR2/3 immunostaining following red nucleus viral injection (n=3). Confocal stack thickness was 1.62 μm.Scales, 5μm.

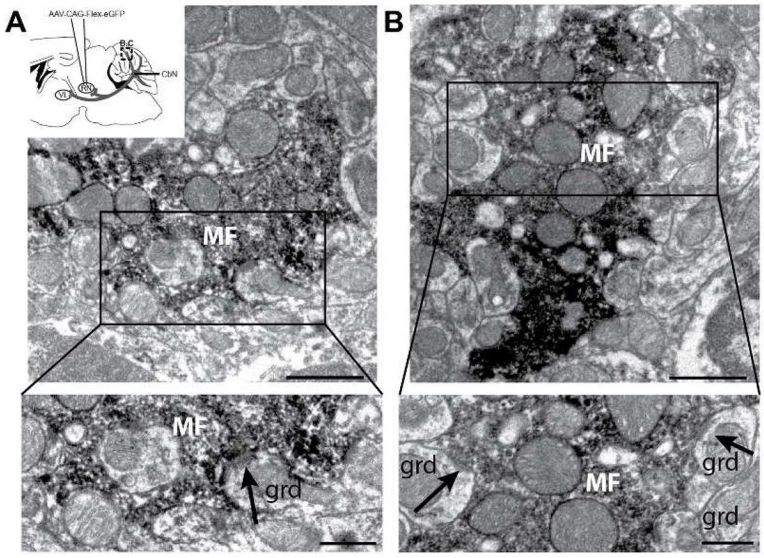

Figure 8.

Nucleocortical terminal active zones are adjacent to granule cell postsynaptic densities. ***A. (inset)*** Schematic diagram showing AAV1-CAG-Flex-eGFP injection to the red nucleus of Ntsr1-Cre mice. Tissue was analyzed for nucleocortical collateral terminal label in the granule cell layer (dashed box). GFP was labeled with DAB for visualization with electron microscopy. ***A, B. (top)*** Electron micrographs showing DAB-labeled mossy fiber rosettes interdigitating with putative granule cell dendrites (grd). Scale = 1μm; ***(bottom)*** Mossy fibers in regions boxed above contained vesicles apposed to postsynaptic density on putative granule cell dendrite (arrows). Scale = 0.5μm.

Table 1

Antibodies Used

Antibody	Immunogen	Manufacturer, Catalog/Lot number, RRID, Host Species	Concentration Used
Synaptic Vesicle Protein 2	Transmembrane glycoprotein of ~95kDa on cytoplasmic side of synaptic vesicles	Developmental Studies Hybridoma Bank, University of Iowa, Cat # sv2, RRID: AB_528480, mouse monoclonal	1:400
Anti-metabotropic Glutamate receptor 2+3	Peptide (NGREVVDSTTSSL) corresponding to 13 c-terminus amino acid of mGluR2 and 3 in rat	Abcam, Cat# ab6438, Lot# GR12051, RRID: AB_10307, rabbit polyclonal	1:500
Anti-Neurogranin	Recombinant rat neurogranin (complete sequence)	Millipore, Cat# AB5620, Lot# 2441899, RRID: AB_91937, rabbit polyclonal	1:500
Anti-GFP	GFP antibody	Abcam, Cat# ab6556, Lot# GR154034-1, RRID: AB_305564, rabbit polyclonal	1:50